Available online at www.sciencedirect.com
ScienceDirect
Polymer 48 (2007) 7008–7016
polymer
www.elsevier.com/locate/polymer

Self-assembling of star-like amphiphilic block copolymers with polyelectrolyte blocks. Effect of pH

Satu Strandman [a], Anna Zarembo [a,*], Anatoly A. Darinskii [b], Benita Löflund [c], Sarah J. Butcher [c], Heikki Tenhu [a]

[a] *Laboratory of Polymer Chemistry, University of Helsinki, P.O. Box 55, FIN-00014 Helsinki, Finland*
[b] *Institute of Macromolecular Compounds, Bolshoi pr. 31, 199004 St. Petersburg, Russia*
[c] *Institute of Biotechnology and Department of Biological and Environmental Sciences, University of Helsinki, P.O. Box 65, FIN-00014 Helsinki, Finland*

Received 7 March 2007; received in revised form 30 September 2007; accepted 1 October 2007
Available online 5 October 2007

Abstract

The self-assembling behaviour of a four-arm amphiphilic star block copolymer, $(PMMA_{73}\text{-}b\text{-}PAA_{143})_4$, with poly(methyl methacrylate) inner blocks and poly(acrylic acid) outer blocks in ratio 1:2 (PMMA:PAA) has been investigated in aqueous solutions as a function of pH by dynamic light scattering and cryo-transmission electron microscopy. At low pH ($pH \leq 5$) the amphiphile forms in the presence of salt both spherical and worm-like micellar aggregates that coexist in solution. At high pH ($pH > 12$) the solution contains mainly spherical micelles and a small number of larger aggregates that have 'pearl-necklace' structure, indicating the disintegration of the worm-like species. In addition to the experiments, computer simulations of the four-arm amphiphilic star block copolymer with the same ratio of the blocks as above were conducted using a coarse-grained model. The simulations predict the formation of the worm-like micellar aggregates at low pH and the spherical ones at high pH. The changes in the morphology of the aggregates are related to the higher degree of ionization of poly(acrylic acid) blocks at high pH and to the swelling of the corona of the micelles by the higher osmotic pressure due to trapped counterions.

Keywords: Amphiphilic star block copolymers; Simulations; Polyelectrolyte

1. Introduction

Amphiphilic block copolymers are capable of self-assembling in solution into nanostructures with various morphologies resembling those observed in nature, such as spherical micelles, worm-like micelles and vesicles [1]. The association behaviour of the amphiphiles depends on the ratios of the hydrophilic and hydrophobic blocks in the block copolymer, as well as on the properties of the solvent, like the composition, pH, or ionic strength, which can induce the self-assembling or trigger the transition between the assembled geometries [2–5]. From the viewpoint of the potential applications of the self-assembled nanostructures, such as nanoreactors [6] and targeted drug delivery [7], it is vital to know how to control the association behaviour. Therefore, there has been growing interest towards investigating the principles of self-association and the stabilisation of the self-assemblies [1]. In addition to linear amphiphilic polymers, aqueous colloidally stable dispersions can be obtained, for example, from spherical polymer brushes prepared by attaching hydrophilic polymers on the surface of nanoparticles or dendrimers [8] or by synthesising amphiphilic star polymers [9].

Amphiphilic star block copolymers may exist in aqueous solutions as single molecules, unimolecular micelles [10,11], or as shown earlier, they may form spherical micelle-like aggregates like their linear analogues [12–15]. In our recent study [16] we reported the self-assembling properties of a four-armed amphiphilic star block copolymer $(PMMA\text{-}b\text{-}PAA)_4$ with poly(methyl methacrylate) inner blocks and poly(acrylic acid) outer blocks in ratio 1:2 (PMMA:PAA). In the

* Corresponding author. Tel.: +358919150346.
E-mail address: anna.zarembo@helsinki.fi (A. Zarembo).

0032-3861/$ - see front matter © 2007 Elsevier Ltd. All rights reserved.
doi:10.1016/j.polymer.2007.10.002

absence of salt, the amphiphile formed spherical multimolecular micelles at low pH (pH = 4.5). However, the addition of salt induced the formation of worm-like micelles upon screening the charges of the polyelectrolyte blocks, resembling the behaviour of linear block copolymers [1,2,17]. The association of the star-like macromolecules resembles also that of charged biopolymers, such as actin, since a balance between attractive and repulsive forces is required for the formation of cylindrical assemblies and can be manipulated by the ionic strength of the solvent [18].

In addition to ionic strength, the solubility of the amphiphile is dependent on pH and thus on the degree of ionization of the polyelectrolyte blocks. Because the electrostatic interactions play an important role in the self-assembling characteristics of the amphiphilic (PMMA-*b*-PAA)$_4$ star block copolymer, in this paper we have focused on investigating its association behaviour in aqueous solutions as a function of pH. The solutions have been probed by dynamic light scattering, and cryo-transmission electron microscopy has been utilised to visualise the morphologies of the aggregates at various pH values. In parallel with the experiments, the self-assembling behaviour of four-arm amphiphilic star block copolymers with polyelectrolyte outer blocks has also been studied using coarse-grain computer simulation. This will be discussed in detail after describing the experimental findings on the self-assembling properties of the polymers.

2. Experimental methods

2.1. Materials

The synthesis and characterization of the four-arm amphiphilic star having block ratio 1:2 (PMMA$_{73}$-*b*-PAA$_{143}$)$_4$ have been described elsewhere [16]. The amphiphilic star block copolymer was synthesised stepwise first by atom transfer radical polymerisation (ATRP) of methyl methacrylate, followed by the block copolymerisation of *tert*-butyl acrylate. The resulting star-like block copolymer of poly(methyl methacrylate) and poly(*tert*-butyl acrylate), (PMMA-*b*-PtBA)$_4$, was further turned amphiphilic by the selective hydrolysis of *tert*-butyl ester groups using trifluoroacetic acid to yield a star with poly(acrylic acid) outer blocks. The number-average molar mass M_n for the (PMMA)$_4$ core is 31,100 g/mol and the polydispersity index (PDI) is 1.30, while the M_n for the (PMMA-*b*-PAA)$_4$ star is 71,200 g/mol and the PDI is 1.33. The values have been determined using size exclusion chromatography (SEC) and ^{1}H NMR spectroscopy.

2.2. Sample preparation

Ultra high quality water purified by ELGA PURELAB Ultra system was used in preparation of all solutions. The solutions were prepared by the direct dissolution of (PMMA-*b*-PAA)$_4$ as lyophilised powder in water with pH 5.8 at room temperature to give 5 mg/ml solutions, which were equilibrated at room temperature for 24 h before use. The polymer was not directly soluble in saline solution and therefore, for dynamic light scattering studies at various pH values, saline solutions were prepared by adding concentrated NaCl (5.0 M) solution to a known volume of aqueous 5 mg/ml polymer solution until the concentration of NaCl was 50 mM, and the pH of the solution (pH = 4.5) was altered by adding concentrated NaOH (5.0 M), during which the ionic strength of the solution increased from 55 mM (pH 5.0) to 80 mM (pH 12.7).

In order to investigate the effect of sample preparation, an additional sample was prepared by the direct dissolution of the polymer in water with pH 12 at room temperature to give 5 mg/ml solution, which was equilibrated as above. After the equilibration, the pH of the polymer solution was adjusted by adding concentrated NaOH (5.0 M). Concentrated NaCl (5.0 M) solution was added to a known volume of the polymer solution, until the ionic strength was 80 mM. The pH of the solution (pH = 11.9) was altered by adding aqueous 5.0 M HCl, during which the ionic strength of the solution increased from 80 mM (pH 11.9) to 113 mM (pH 4.6). The sample was equilibrated for 24 h at 20 °C prior to the measurements.

2.3. Instrumentation

2.3.1. Light scattering

Dynamic light scattering (DLS) measurements were conducted with a Brookhaven Instruments BI-200SM goniometer and a BI-9000AT digital correlator. Ar laser (LEXEL 85, $\lambda = 488.0$ nm) was used as a light source. In dynamic light scattering, the time autocorrelation function of scattered light intensity

$$G_2(t) = \langle I(0)I(t)\rangle \quad (1)$$

was collected in self-beating mode. The correlation function was analyzed by the inverse Laplace transform program CONTIN to obtain distributions of relaxation times τ, of corresponding correlation functions of electric field, $G_1(t)$, or distributions of hydrodynamic radii R_h. The values of refractive index and viscosity of water were used for the aqueous solution. The temperature was 20 °C and the range of studied scattering angles was 35°–140°. The equipment was calibrated using toluene.

2.3.2. Cryo-transmission electron microscopy

Aliquots (3 μl) of (PMMA-*b*-PAA)$_4$ at 5 mg/ml in aqueous NaCl were pipetted onto 400 mesh copper grids covered with a holey carbon film (Quantifoil R 2/2) and vitrified by plunging into liquid ethane [19]. Samples were maintained at −180 °C in a Gatan 626 cryoholder whilst images were recorded on an FEI Tecnai F20 field emission gun transmission electron microscope (Electron Microscopy Unit, Institute of Biotechnology, University of Helsinki) at 200 kV under low-dose conditions at a nominal magnification of 50,000× on Kodak SO163 film or of 68,000× on a Gatan 4 k × 4 k US4000 CCD camera. Micrographs that were free of drift and astigmatism were digitized at 7 μm intervals on a Zeiss Photoscan TD scanner resulting in a nominal sampling of 1.4 Å pixel^{-1},

while the sampling of the digital images obtained by the CCD camera was 2.21 Å pixel^{-1}.

3. Results and discussion

3.1. Light scattering and cryoTEM

The investigated amphiphilic star block copolymer, $(PMMA_{73}$-*b*-$PAA_{143})_4$, is illustrated in Scheme 1. Due to the high content of poly(acrylic acid) (PMMA:PAA 1:2), the polymer is soluble in water, forming spherical or slightly elongated micelle-like aggregates in the absence of salt [16]. However, the solubility is dependent on pH as the polymer precipitates upon the addition of HCl and it does not dissolve in water with pH < 4.5. The micellisation of the amphiphilic star is in agreement with the experimental results and simulations reported for similar systems [12–14]. The polymer solution (pH = 4.5) became opaque upon the addition of salt because of the presence of large, worm-like micelles coexisting with the spherical ones, which has been verified by Kratky analysis of the light scattering data [16] and by cryoTEM (Fig. 1). When the pH of the saline 5 mg/ml solution of the amphiphile is increased by the addition of NaOH, the solution becomes less cloudy and the normalised light scattering intensity of the solution decreases (Fig. 2a), indicating the decrease in the average molar mass or the density of the aggregates. The distributions of hydrodynamic radius of 5 mg/ml solution at pH 5.0 and pH 12.7 (Fig. 2b) show that the polydispersity of the sample is high, being slightly higher at lower pH, which is also represented by the higher curvature of the correlation

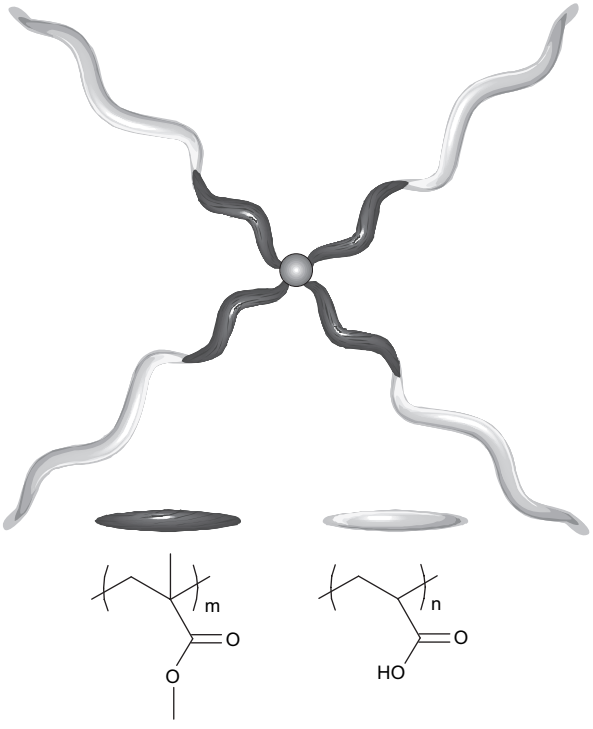

Scheme 1. Structure of the investigated star block copolymer $(PMMA_{73}$-*b*-$PAA_{143})_4$.

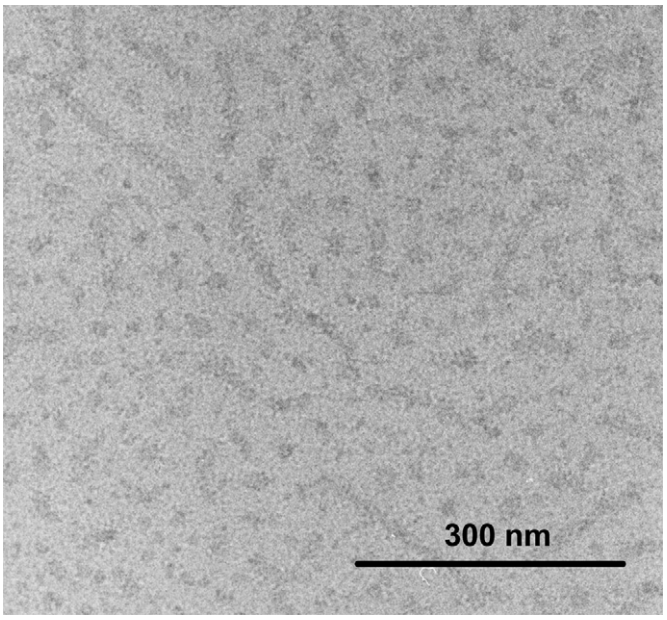

Fig. 1. Representative cryo-transmission electron micrograph of (PMMA-*b*-$PAA)_4$ star polymer in 5 mg/ml aqueous NaCl solution having ionic strength 100 mM (pH 4.5, underfocus 8.4 μm).

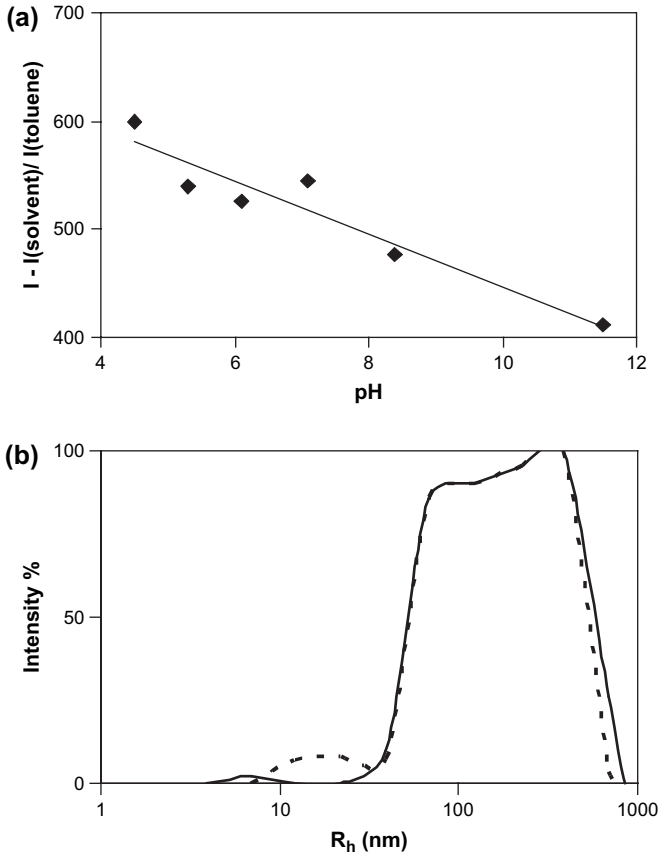

Fig. 2. (a) Normalised scattering intensity as a function of pH. The line has been added as the guide for eye. (b) Distributions of hydrodynamic radius at pH 5.0 (dashed line) and at pH 12.7 (solid line) measured at 35° scattering angle for aqueous 5 mg/ml solution of (PMMA-*b*-$PAA)_4$.

function of electric field at pH 5.0 (available in Supplementary data). According to the size distributions given by CONTIN, the solution contains large aggregates that along with the high polydispersity make it difficult to estimate the molar mass and the density of the species. There is a small difference in the shape of the autocorrelation functions of scattered light at the measuring angle 35° (Fig. 3) indicating that the solution of the amphiphile consists of larger aggregates at pH 5.0 than at pH 12.7, thus explaining the higher turbidity at low pH. Since the large species dominates the scattering behaviour, the difference is not observed at the measuring angle 90°, demonstrated by the identical autocorrelation functions shown in the inset of Fig. 3. At high pH, the light scattering behaviour of the samples does not depend on the way of sample preparation, as the autocorrelation functions both at 90° and 35° are identical for the sample prepared at low pH and titrated to pH 12.7 and for the one prepared at high pH (pH 11.9). When pH of the latter sample is decreased to 4.6, the difference between the autocorrelation functions at 35° (available in Supplementary data) and lower scattering intensity indicate a smaller fraction of large scatterers. Nevertheless, cryoTEM micrographs still show the coexistence of spherical and worm-like micelles at pH 4.6. It may be concluded that the formation of worm-like micelles is reversible.

Because of the polydisperse samples and the minor differences in the light scattering data at two different pH values, cryo-transmission electron microscopy was utilised to obtain further information of the sizes and shapes of the aggregates at high pH. The micrographs of the 5 mg/ml solution of the amphiphile at pH 12.7 (Figs. 4–6, ionic strength $I = 80$ mM) show that the sample mainly consists of spherical micelles, but there are also some larger elongated aggregates having loose 'pearl-necklace' structure visible in Figs. 5 and 6. In accordance with the light scattering results, the fraction of elongated or worm-like species is lower than at pH 4.5 (Fig. 1, $I = 100$ mM). The micrographs at two different ionic strengths are comparable with each other, as according to

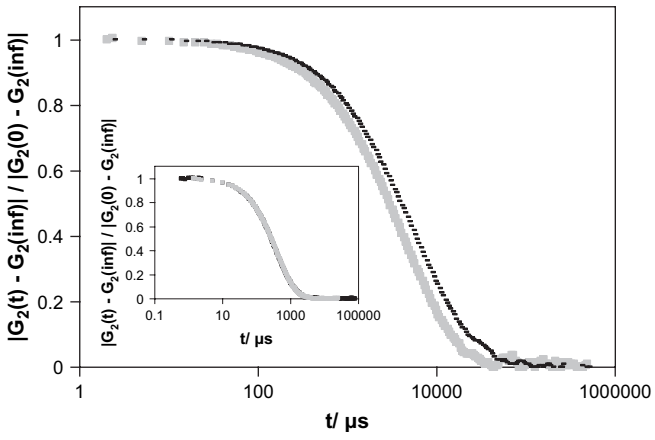

Fig. 3. Normalised autocorrelation functions of the intensity of scattered light, $G_2(t)$, measured at 35° scattering angle for aqueous 5 mg/ml solution of (PMMA-*b*-PAA)$_4$. Black symbol (■) corresponds to pH 5.0 and gray one (▒) to pH 12.7. The inset shows overlapping autocorrelation functions of the same samples at 90° scattering angle.

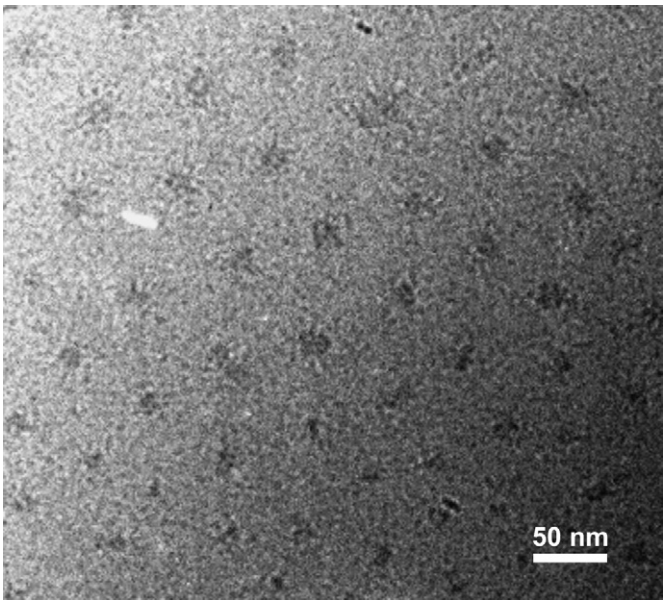

Fig. 4. A cryo-transmission electron micrograph of (PMMA-*b*-PAA)$_4$ star polymer in 5 mg/ml aqueous NaCl solution having pH 12.7 and ionic strength 80 mM (underfocus 7 µm). The image shows a uniform distribution of micelle-like aggregates.

the dynamic light scattering studies, there was no considerable difference in the shape of the correlation functions of electric field at the ionic strengths $I = 50–100$ mM (data not shown here). This also indicates that the major differences in micellar morphologies are due to the change in pH rather than in ionic strength.

The micrograph in Fig. 4 represents a uniform distribution of spherical micelles, which can be used in estimating their dimensions. According to the micrograph, at pH 12.7 the diameter of the dark area of the spherical micelles is 25 ± 6 nm and the distance between the centres of the spheres is 73 ± 8 nm, whereas at pH 4.5 the diameter was 19 ± 3 nm, being within the error of the value at pH 12.7 [16]. Assuming that the spherical micelles touch each other in the uniform distribution, we may calculate the maximum radius of the corona using the distance between the cores, which gives R(corona) = 24 nm and R(corona)/R(core) = 1.92. For the time being, this value is surprisingly close to the block ratio PAA/PMMA = 1.95. Nevertheless, the micelles may be kept apart by the repulsion between the charged polyelectrolyte shells thus preventing their close contact and hence the actual diameter of the micelles may be smaller than their mutual distance.

Fig. 5 shows clearly the radiating arms from the cores of the spherical micelles as well as from the larger aggregates in the solution. This 'fuzziness' or roughness in the images makes it difficult to estimate the boundaries of the aggregates, since there is a contrast between the compact PMMA core of the micelles and the less dense corona of the hydrophilic PAA blocks. The enlargement of part of Fig. 5 shows beautifully the star-like structure of the spherical micelle. It would be tempting to consider that the inset would represent a single star, so called 'unimolecular micelle', instead of an aggregate.

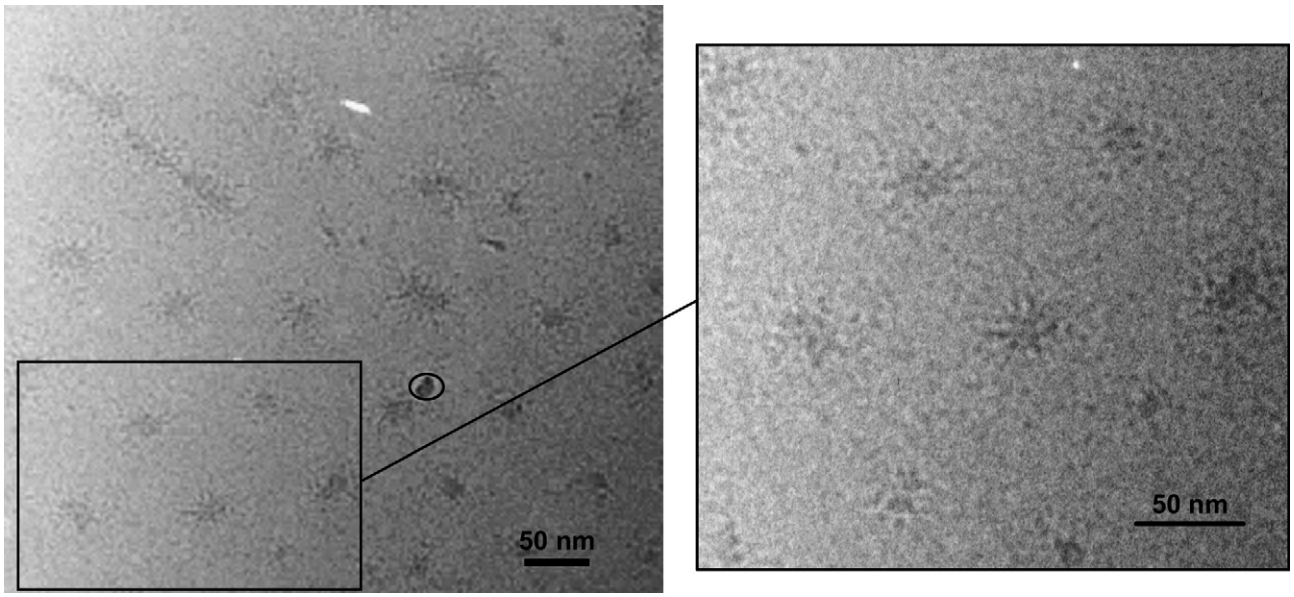

Fig. 5. A cryo-transmission electron micrograph of (PMMA-*b*-PAA)$_4$ star polymer in 5 mg/ml aqueous NaCl solution having pH 12.7 and ionic strength 80 mM (underfocus 7 μm). The defect in the image from ice has been circled. The enlargement of part of the micrograph shows micelles displaying radiating arms.

However, we have reported earlier that the hydrodynamic diameter of the hydrophobic precursor of the amphiphilic star, (PMMA$_{73}$-*b*-PtBA$_{143}$)$_4$, was 15.8 nm in THF, a good solvent for both blocks. Since in the aqueous environment the PMMA core of the amphiphile is collapsed, the diameter of the dense core of a unimolecular micelle would be considerably lower than this value, which is not in correspondence with the value obtained from the micrograph [16].

The 'pearl-necklace' structure of a worm-like aggregate at pH 12.7 can be observed in the micrograph shown in Fig. 6.

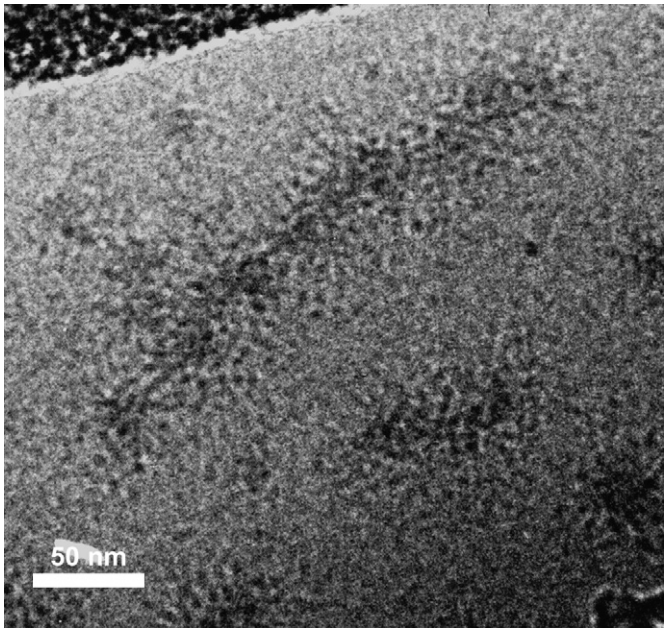

Fig. 6. An enlargement of the cryo-transmission electron micrograph of (PMMA-*b*-PAA)$_4$ star polymer in 5 mg/ml aqueous NaCl solution having pH 12.7 and ionic strength 80 mM (underfocus 7 μm). The image shows the 'pearl-necklace' structure of a disintegrated worm-like micelle.

A large worm-like species seems to be composed of smaller spherical species. None of the worm-like micelles in the cryo-TEM micrographs of the solution at pH 4.5 exhibited this type of structure, but were intact. The 'pearl-necklace' structure could arise from the disintegration of the larger aggregates due to the increased repulsion or swelling within the polyelectrolyte corona, as suggested by the decrease in the light scattering intensity upon increasing pH. The disintegration of large aggregates also explains why the fraction of spherical micelles is higher at high pH. The observation is in accordance with those described for linear amphiphilic block copolymers having weak polyelectrolyte as a hydrophilic block [20,21]. According to Zhang and Eisenberg [20] who have described the behaviour of linear PS–PAA block copolymers with a short hydrophilic block, the formation of various micellar morphologies in the aqueous solutions of amphiphilic block copolymers is governed by the extension of the hydrophobic blocks in the micellar core, the surface tension between the core and the solvent, and the repulsion between the hydrophilic chains in the corona. Increasing the aggregate size upon decreasing electrostatic repulsion is thermodynamically favorable in order to reduce the interfacial area between the solvent and the hydrophobic core [17]. When the pH of the solution is increased by the addition of NaOH the degree of ionization of the polyelectrolyte blocks increases. As a result, the size of the aggregates decreases due to the stronger repulsion between the ionized groups in the coronas or due to the higher osmotic pressure of counterions within the ionized polyelectrolyte corona.

4. Simulation

Next, our aim has been to find out how much information on this complex system may be derived using theoretical simulation methods. The results of simulations of pH effect on the

morphology of micelles formed by the star copolymers will be presented. There are several works devoted to the simulation of neutral block copolymers of different architectures: diblock, triblock and stars in selective solvents [22,23]. It has been shown that by changing the ratio of the lengths of the blocks it is possible to obtain different morphologies of micelles. However, there are only few works addressing the simulation of block copolymer solutions with polyelectrolyte blocks. For example, Roger et al. [23] simulated isolated spherical star-branched micelles with polyelectrolyte coronas. Effect of the strength of the Coulomb coupling on the distribution of counterions was considered. To our best knowledge no articles have addressed the effect of pH on the morphology of micelles formed by copolymers with polyelectrolyte block by simulations.

4.1. Model

As a model for PMMA-*b*-PAA star copolymers we considered a coarse-grained bead–rod model of flexible polymer chains [24]. The chains consist of two types of beads: hydrophobic non-charged ones representing certain structural units of PMMA and hydrophilic ones which may carry negative charges, the latter one representing the structural units of PAA.

As in the experiments above we consider four-armed stars. Every arm of a star consists of 7 hydrophobic and 14 hydrophilic beads, so that the ratio of block lengths is the same as in the experimentally studied system. Every bead represents an effective unit of interaction. To save computer time we have chosen the number of repeating units in the effective unit to be equal to 10, which is slightly higher than the number of units in a Kuhn segment (about 6 for PMMA and PAA). We believe this will not significantly affect the results. The arms have one common bead, which is identical to a hydrophobic PMMA bead (Scheme 2). The simulated system is a dilute solution of such stars. In addition to polymer stars the simulation box contains also oppositely charged small mobile counterions.

The simulation was performed by the stochastic dynamics method [24], i.e. solving the Langevin equations for all particles in the system (polymer beads and counterions) simultaneously. The solvent is considered as an effective viscous medium and a heat bath. All particles have the same friction coefficient.

The excluded volume interaction between any non-bonded particles is described by a repulsive Lennard–Jones potential [25]:

$$U(r) = \begin{cases} 4\varepsilon\left[\left(\frac{\sigma}{r}\right)^{12} - \left(\frac{\sigma}{r}\right)^{6} + \frac{1}{4}\right], & r \le 2^{1/6}\sigma \\ 0, & r > 2^{1/6}\sigma \end{cases} \quad (2)$$

where $\sigma = \varepsilon = 1$ for polymer beads, and $r_0 = 2^{1/6}\sigma$ is a cutoff distance. For counterions the parameter σ is smaller ($\sigma = 0.2$). In addition, non-bonded chain beads interact with each other by an attractive Yukawa-type potential [24]:

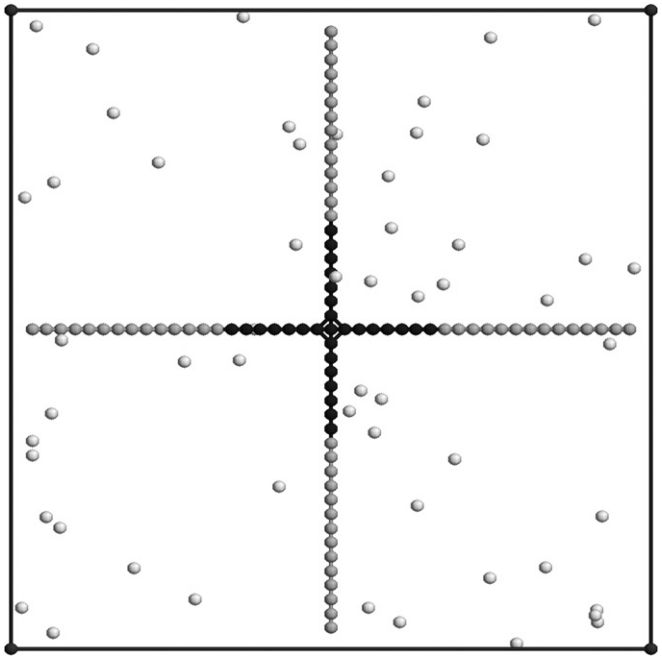

Scheme 2. Layout of the course-grained model of a four-arm star with counterions.

$$U(r) = \begin{cases} -\varepsilon\left(\frac{\sigma}{r}\right)\left[1 - \left(\frac{r}{r_c}\right)^2\right]^2, & r \le r_c \\ 0, & r > r_c \end{cases} \quad (3)$$

with the cutoff distance $r_c = 2.8\sigma$.

Chain beads comprising the copolymer chains are connected by rigid bonds of a fixed length $l = \sigma$.

Similar to Ref. [26] we use the solvent accessible surface area (SASA) potential [26] to describe hydrophobic–hydrophilic interactions of polymer chains with the solvent:

$$U(s) = A_i S_i \quad (4)$$

were S_i is the surface area for each particle, accessible to solvent. The area is calculated according to Lee and Richards procedure [27]. In our simulations we use a rolling probe particle with $\sigma = 0.5$. The strength of the hydrophobic and the hydrophilic interactions are characterized by coefficients A_i. We have chosen the values of A_i similar to those used for lattice MC simulation [28] of diblock copolymers in water solution: $A_i = 4.0$ for hydrophobic and $A_i = -1.0$ for hydrophilic beads.

Electrostatic interactions between charged particles are described by the Coulomb potential:

$$U_C = \frac{1}{4\pi\varepsilon_o\varepsilon_r}\sum_m \sum_{i\neq j}^{N} \frac{q_i q_j}{\left|\boldsymbol{r}_{ij} + \boldsymbol{m}L_{box}\right|} \quad (5)$$

where $\mathbf{r}_{ij} = \mathbf{r}_i - \mathbf{r}_j$, $\boldsymbol{m}$ is identification of a particular image cell, L_{box} is side length of periodic cell, q_i is a charge of a given particle (in e units), and $l_B = e^2/4\pi\varepsilon_0\varepsilon_r k_B T$ is a Bjerrum length characterizing the intensity of electrostatic interactions. Its value in water is equal to 7.14 Å. We have set it equal to unity in our simulations.

The equations of motion are solved iteratively using a Newtonian iteration procedure with the time step $t = 0.01\sigma(m/\varepsilon)^{1/2}$ (see Ref. [29] for more technical details). The unit of time in the simulation is defined by $\tau = \sigma(m/\varepsilon)^{1/2}$, length are in σ units. In the following, the reference temperature $T = \varepsilon/k_B$ is equal to unity.

Due to the periodic boundary condition the highly optimized particle mesh Ewald (PME) method [30,31] for the correct calculations of the electrostatic interactions was used. The cutoff distance for the electrostatic interaction and other calculation parameters are taken similar to those in a previous study on a nearly similar system [24].

Here we will consider two extreme cases corresponding to low and high pH where worm-like and spherical micelles were observed, correspondingly. Due to the time consuming calculations of electrostatic interactions we have chosen to restrict ourself to the simplest possible model, which still captures the essential behaviour of the system.

It is well known that the morphology of micelles in block copolymer solutions with weak polyelectrolyte blocks is determined both by the degree of ionization of the blocks (which depends on pH) and by the salt concentration [32]. The increase of the first factor leads to the swelling of the micelle corona and therefore to the decrease of the aggregation number and to the preference of the spherical morphology in comparison to the worm-like one. However, the increase of the salt concentration leads to an effective screening of the electrostatic interactions (in the mean-field approximation to the decrease of the Debye radius) and makes the worm-like morphology more favorable. To estimate the balance of these factors in the present case let us make some simple estimations of the concentration of salt ions and counterions in solution. Experiments in saline solutions of the (PMMA-*b*-PAA)$_4$ stars were made at the salt concentrations of 0.05–0.1 M. Taking into account the degree of the dissociation of *NaCl* in water (approx. 0.95) the resulting number concentration of salt molecules is $3–6 \times 10^{19}$ ml^{-1}. This corresponds to a Debye radius of $\sim$10 Å. Let us estimate now the number concentration of counterions H^+ in a 5 mg/ml at different pHs. At low pH = 4–5 the degree of dissociation of PAA is small (about 0.1). Therefore the number concentration of counterions (for PAA blocks) is less than 2×10^{19} ml^{-1}, i.e. less than that of salt ions. In this regime the main factor is a screening of electrostatic interactions between rare charges in the corona chains. For our coarse-grained model the Debye radius occurs to be of the order of unity and close to the radius of repulsive excluded volume interactions. Therefore for the simulation of this regime it is reasonable to use the model with hydrophilic but neutral PAA beads.

At high pH = 12 and in the presence of salt the degree of ionization of PAA blocks is close to unity. In this case the concentration of counterions is significantly larger (about 2.5×10^{20} ml^{-1}) than that of salt ions and the main factor determining the morphology is the swelling of corona due to the osmotic pressure of trapped counterions.

Therefore for this case it is reasonable to use the model with charged PAA beads and explicit counterions. The overall number of counterions in the simulation cell is equal to that of charged PAA beads.

4.2. Preparation of the system

The simulation cell contained 100 four-arm stars. Every arm consist of 7 PMMA beads and 14 PAA beads, which amounts to 85 beads per star. The total number of polymer beads was $N = 8500$. The volume V of the simulation box was chosen such that the number density of polymer segments $\rho = N/V = 0.005$ corresponds to the experimental polymer concentration 5 mg/ml. To preserve the electroneutrality of the system in the case of charged PAA beads (with $q = -1$) the cell contained also 5600 counterions (with $q = +1$) equal to the number of PAA beads.

In the initial state the system is fully disordered. Equilibration of the systems was carried out using *NVT* ensemble during 5×10^5 steps. The system was considered as equilibrated when the aggregation number distribution of micelles did not change appreciably during sufficiently long time. Following the equilibration phase a production run of 5×10^5 time steps was performed and the structural characteristics of the systems were determined.

4.3. Simulation results

In all cases the micelle formation was observed. The snapshots illustrating the morphology of micellar aggregates obtained under different conditions are shown in Fig. 7. For the model corresponding to low pH (PAA beads are non-charged) we obtained single worm-like micelles with an aggregation number of 100. The micelles consist of dense core and more loose corona. Mean-squared end-to-end distance of hydrophobic (H) blocks $<h_H^2>^{0.5}$ representing PMMA blocks in the core and the hydrophilic (P) blocks $<h_P^2>^{0.5}$ representing PAA blocks in the corona are equal to 3.3 and 7.5, respectively. To compare the conformation of chains in the core and corona with those of free chains we have simulated a number of single linear homopolymer chains composed of 7 hydrophobic and 14 hydrophilic beads and calculated their

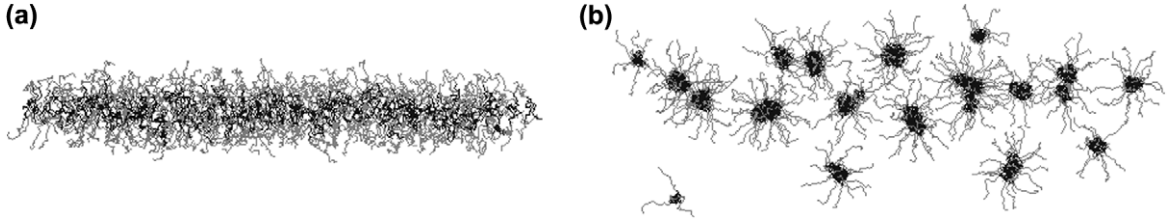

Fig. 7. Snapshots of the simulated systems at low pH (non-charged) (a) and at high pH (charged) (b); shown without counterions.

unperturbed mean-squared end-to-end distances in the globular $<h^2_{H\ single}>$ and swollen $<h^2_{P\ single}>$ states. The ratio of $<h^2_H>^{0.5}/<h^2_{H\ single}>^{0.5} = 1.7$ and $<h^2_P>^{0.5}/<h^2_{P\ single}>^{0.5} = 1.14$. The comparison with the contour length L of chains gives the degree of stretching $<h^2_H>^{0.5}/L = 0.3$ and $<h^2_P>^{0.5}/L = 0.5$ correspondingly.

For the model corresponding to the solution of stars at high pH (all hydrophilic beads are charged) much smaller micelles with a broad distribution of aggregation numbers (Fig. 7b) were observed. The average aggregation number is equal to 5. The majority of micelles are of spherical shape. Only one of the micelles with aggregation number of 11 is nonspherical. Probably this structure is not equilibrated enough and much more longer simulation time is necessary for its equilibration. The micelles contain again a dense core but the corona chains are more stretched than in the previous case. The conformation of hydrophobic blocks with $<h^2_H>^{0.5} = 3.4$ in the core of spherical micelles is practically the same as in the worm-like micelle. However, hydrophilic blocks are two times more stretched ($<h^2_P>^{0.5} = 12.3$) than in the worm-like micelle with non-charged corona beads. The degree of stretching $<h^2_P>^{0.5}/L = 0.95$ is close to the maximum.

Two mechanisms of the stretching of corona chains in micelles with polyelectrolyte blocks are discussed in the literature (see for example Refs. [22,32]). The first one is attributed to the repulsion of charged chain units in the corona. It is expected that at very low total counterion concentrations the concentration of counterions close to the corona is decreased, due to entropic effects, compared to the bulk leading to a net effective charge of the corona. The second possible mechanism is the swelling of the corona due to the osmotic pressure of counterions. In this case the majority of counterions are trapped into the corona. The analysis of our data shows that more than 70% of counterions are trapped in the coronas of the micelles and therefore the swelling mechanism is responsible for the stretching of corona chains in our case. As an example we show (Fig. 8) the distribution of counterions for two micelles both consisting of four stars.

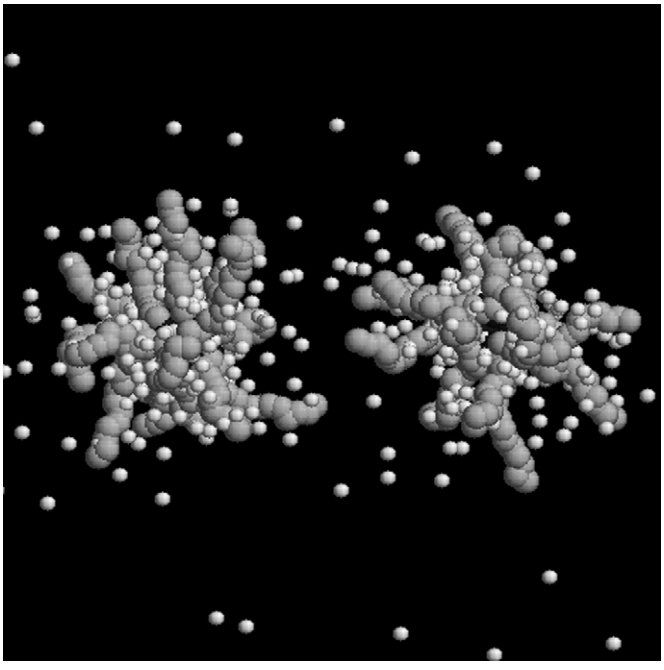

Fig. 8. Snapshot of two micelles both consisting of four stars; high pH, shown with counterions.

The specific energy of electrostatic interactions between charged beads and counterions in corona occurs to be much less than kT and two orders of magnitude less than that of Van der Waals interactions of these particles. This confirms our conclusion about the osmotic pressure mechanism of corona swelling.

5. Conclusions

The self-assembling of amphiphilic (PMMA-*b*-PAA)$_4$ star diblock copolymer in saline aqueous solutions was investigated upon the change of the pH both experimentally and by computer simulation. According to the dynamic light scattering and cryoTEM studies, the polymer forms both spherical and worm-like micelle-like aggregates at low pH. When pH is increased, the worm-like species disintegrates into smaller spherical micelles, which is in agreement with the results of coarse-grained computer simulations using the same architecture and the length ratio of hydrophobic and hydrophilic blocks. The changes in the morphology of the aggregates at high pH are due to the higher degree of ionization of polyelectrolyte blocks and swelling of the corona owing to the higher osmotic pressure by trapped counterions.

Acknowledgements

S. Strandman wishes to thank Finnish National Graduate School in Nanoscience (NGS-NANO) for financial support. A. Zarembo thanks the Academy of Finland for funding. A. Darinskii is grateful to the RFBR (grant 05-03-32450) and to Magnus Ehrnrooth fund for financial support. The authors wish to thank Dr. Vladimir Aseyev for helpful discussions and Prof. Pavel Khalatur for providing the computer code.

Appendix. Supplementary data

The correlation functions of electric field and corresponding autocorrelation functions at 35° measuring angle for 5 mg/ml solutions of the amphiphilic star block copolymer (PMMA-*b*-PAA)$_4$. Supplementary data associated with this article can be found, in the online version, at doi:10.1016/j.polymer.2007.10.002.

References

[1] Rodríguez-Hernández J, Chécot F, Gnanou Y, Lecommandoux S. Prog Polym Sci 2005;30:691–724.
[2] Discher DE, Eisenberg A. Science 2002;297:967–73.
[3] Choucair A, Lavigueur C, Eisenberg A. Langmuir 2004;20:3894–900.
[4] Zhang L, Eisenberg A. Macromolecules 1999;32:2239–49.
[5] Ma Q, Remsen EE, Clark Jr CG, Kowalewski T, Wooley KL. Proc Natl Acad Sci USA 2002;99:5058–63.

[6] Boontongkong Y, Cohen RE. Macromolecules 2002;35:3647–52.
[7] Dalhaimer P, Engler AJ, Parthasarathy R, Discher DE. Biomacromolecules 2004;5:1714–9.
[8] Guo X, Ballauff M. Langmuir 2000;16:8719–26.
[9] Heise A, Hedrick JL, Frank CW, Miller RD. J Am Chem Soc 1999;121:8647–8.
[10] Gitsov I, Fréchet JMJ. J Am Chem Soc 1996;118:3785–6.
[11] Yoo M, Heise A, Hedrick JL, Miller RD, Frank CW. Macromolecules 2003;36:268–71.
[12] Narrainen AP, Pasqual S, Haddleton DM. J Polym Sci Part A Polym Chem 2002;40:439–50.
[13] Kim KH, Cui GH, Lim HJ, Huh J, Ahn CH, Jo WH. Macromol Chem Phys 2004;205:1684–92.
[14] Huh J, Kim KH, Ahn CH, Jo WH. J Chem Phys 2004;121:4998–5004.
[15] Whittaker MR, Monteiro MJ. Langmuir 2006;22:9746–52.
[16] Strandman S, Hietala S, Aseyev V, Koli B, Butcher SJ, Tenhu H. Polymer 2006;47:6524–35.
[17] Zhang L, Eisenberg A. J Am Chem Soc 1996;118:3168–81.
[18] Tang JX, Janmey PA. J Biol Chem 1996;271:8556–63.
[19] Adrian M, Dubochet J, Lepault J, McDowall AW. Nature 1984;308:32–6.
[20] Zhang L, Eisenberg L. Macromolecules 1996;29:8805–15.
[21] Förster S, Abetz V, Müller A. Adv Polym Sci 2004;166:173–210.
[22] Hamley IW. Block copolymers in solution: fundamentals and applications. New York: Wiley; 2005. p. 33–45.
[23] Roger M, Guenoun P, Muller F. Eur Phys J 2002;9:313–26.
[24] Khalatur PG, Khokhlov AR, Mologin DA, Reineker P. J Chem Phys 2003;119:1232.
[25] Allen MP, Tildesley DJ. Computer simulation of liquids. Oxford, UK: Clarendon; 1990.
[26] Wesson L, Eisenberg D. Protein Sci 1992;1:227.
[27] Lee B, Richards FM. J Mol Biol 1971;55:379.
[28] Termonia Y. J Polym Sci Part B 2002;40:890.
[29] Khalatur PG, Balabaev NK, Pavlov AS. Mol Phys 1986;59:753.
[30] Darden TA, York DM, Pedersen LG. J Chem Phys 1993;98:10089.
[31] Essmann U, Perera L, Berkowitz ML, Darden T, Lee H, Pedersen LG. J Chem Phys 1995;103:8577.
[32] Borisov OV, Zhulina EB. Macromolecules 2003;36:10029.